Available online at www.sciencedirect.com
SCIENCE DIRECT
Vacuum 80 (2006) 1042–1045
VACUUM
SURFACE ENGINEERING, SURFACE INSTRUMENTATION & VACUUM TECHNOLOGY
www.elsevier.com/locate/vacuum

Short communication

Structural and optical properties of GaN films grown on GaAs substrates by molecular beam epitaxy

O. Maksimov[a,*], Y. Gong[b], H. Du[c], P. Fisher[c], M. Skowronski[c], I.L. Kuskovsky[b], V.D. Heydemann[a]

[a]*Electro-Optics Center, Pennsylvania State University, Freeport, PA 16229, USA*
[b]*Department of Physics, Queens College of City University of New York, Flushing, NY 11367, USA*
[c]*Department of Materials Science and Engineering, Carnegie Mellon University, Pittsburgh, PA 15213, USA*

Received 24 September 2005; accepted 3 January 2006

Abstract

GaN films are grown on [0 0 1] GaAs substrates by plasma-assisted molecular beam epitaxy using a three-step process that consists of a substrate nitridation, deposition of a low-temperature buffer layer, and a high-temperature overgrowth. X-ray diffraction and transmission electron microscopy indicate that this method promotes prismatic growth of c-oriented α-GaN. Photoluminescence studies show that the emission from cubic β-GaN inclusions dominates the spectrum.

Keywords: Molecular beam epitaxy; GaN; GaAs

GaN materials are technologically important for a variety of device application [1,2]. They are ideal candidates for fabrication of high power microwave devices, high-frequency field effect transistors, high electron mobility transistors, light emitters and detectors operating in the visible to UV spectral range. High-quality hexagonal GaN (α-GaN) films and heterostructures are usually grown either by metal organic chemical vapor deposition (MOCVD) or by molecular beam epitaxy (MBE) on sapphire (α-Al_2O_3) and 6H-SiC substrates [3,4]. Growth on [0 0 1] GaAs is much less studied, although these substrates provide several advantages, such as, low cost, easy cleavage along [0 1 1] direction, closer thermal expansion coefficient matching, and possibility to stabilize cubic β-GaN.

When GaN is grown on GaAs, an optimization of the GaAs surface, by growing a GaAs buffer layer, always precedes GaN deposition [5–7]. However, As gets incorporated into the GaN alloy, degrading luminescent and transport properties of the film [8,9]. Therefore, it is of interest to explore GaN growth in the As-free environment. We have previously observed that direct deposition on a thermally desorbed GaAs results in the growth of a polycrystalline poorly oriented α-GaN containing misoriented domains and large cubic inclusions. However, a significant improvement of the crystallinity is achieved by adopting the growth procedure that consists of a substrate nitridation, deposition of a low-temperature buffer layer, and epitaxial overgrowth at elevated temperature. These steps effectively suppress misorientation and improve morphology of the film [10].

Here we present a detailed study on the structural and optical properties of the GaN grown under these conditions. The crystalline quality and the morphology of the films are examined with X-ray diffraction (XRD), transmission electron and atomic force microscopes (TEM and AFM). Optical properties are evaluated with the continuous wave photoluminescence (PL).

The samples are fabricated in a custom-built MBE system equipped with a Ga effusion cell, a radio frequency excited nitrogen plasma source, a retractable ion gauge for flux calibration, and a reflection high-energy electron diffraction (RHEED) system. For the growth we use

*Corresponding author. Tel.: +1 724 295 6624; fax: +1 724 295 6617.
E-mail address: Maksimov@netzero.net (O. Maksimov).

0042-207X/$ - see front matter © 2006 Elsevier Ltd. All rights reserved.
doi:10.1016/j.vacuum.2006.01.001

semi-insulating epi-ready [0 0 1] GaAs substrates indium mounted to molybdenum holders. To prevent As incorporation, the oxide layer is desorbed at 500 °C in the absence of As flux. The GaAs wafer is exposed every 30 s to sub-monolayer Ga pulses to facilitate oxide desorption through the conversion of Ga_2O_3 to a more volatile Ga_2O [11]. The progress of oxide removal is monitored in situ with RHEED.

Fig. 1 shows a plot of specular RHEED intensity as a function of time. Prior to wafer exposure to Ga flux, we observe a diffused halo pattern typical for the amorphous oxide layer. This layer is stable at 500 °C since there is no significant change in the RHEED pattern if the wafer is kept at this temperature for a prolonged time. Initially, Ga pulses result in a slow increase of specular RHEED intensity due to the thinning of the oxide layer. Then, after a set ~15 pulses, we start to observe a different behavior, with spot intensity immediately dropping in the response to Ga exposure and slowly recovering to a higher level during the pulses. This behavior is due to the formation of oxide-free patches at the wafer surface and migration of Ga to the remaining oxide patches [11]. We terminate Ga deposition at this point to prevent oversupply of Ga and formation of droplets. This process results in a slightly distorted GaAs surface characterized by a (2×2) reconstruction. Kikuchi lines are clearly evident, indicating that GaAs surface is free of oxide layer, Fig. 2A.

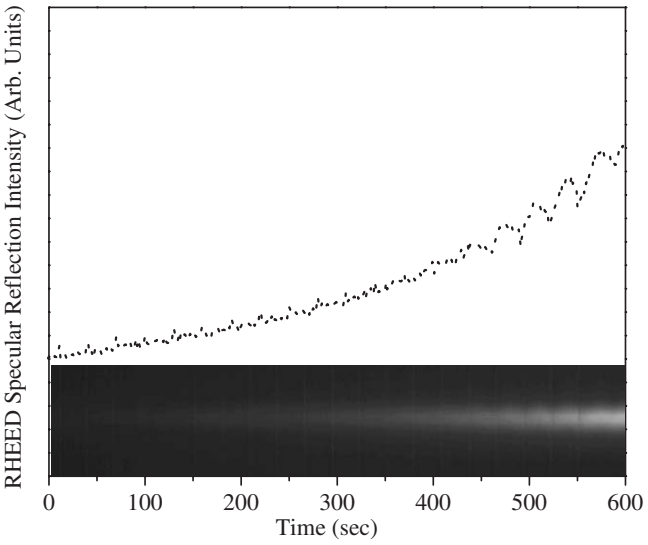

Fig. 1. Time dependence of a specular RHEED reflection.

Next, we decrease wafer temperature to 400 °C to perform substrate "nitridation". Surface reconstruction disappears during the first few minutes of wafer exposure to nitrogen plasma suggesting formation of an amorphous GaAsN layer. We observe an arc pattern after approximately 5 min indicating development of a preferred orientation in a disordered layer, Fig. 2B. Spot-like features with hexagonal symmetry develop by the end of nitridation. Annealing at 600 °C sharpens diffraction spots demonstrating recrystallization of α-GaN phase, Fig. 2C. The diffraction spots are relatively broad signifying that very defective GaN layer forms at the beginning. However, they become significantly sharper and elongated during the growth of a relatively thin (50-nm) buffer layer, indicating that final GaN film has a better crystalline quality and a smoother surface. Finally, we raise wafer temperature to

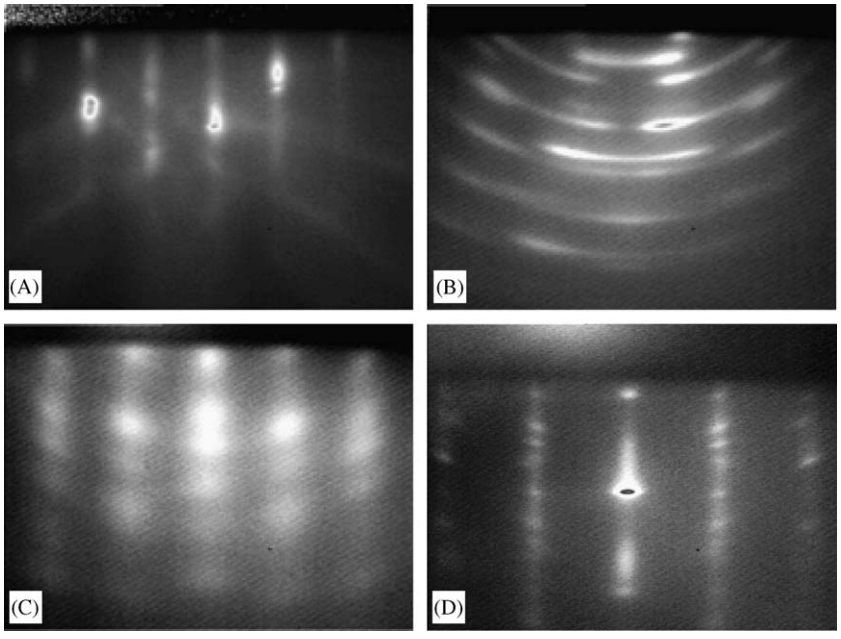

Fig. 2. RHEED patterns for: (A) GaAs substrate after oxide desorption, (B) GaAs substrate after 5 min of nitridation, (C) nitridated GaAs substrate after annealing at 600 °C and (D) GaN film grown at 750 °C.

750 °C for further GaN growth. When the growth is initiated, we observe a streaky (1 × 1) reconstruction, Fig. 2D.

A XRD $\theta-2\theta$ scan of GaN film grown under these conditions is shown in Fig. 3. The main diffraction peak is $\langle 0\,0\,0\,2\rangle$ α-GaN. A very weak $\langle 0\,0\,2\rangle$ β-GaN diffraction is also present. AFM images, Fig. 4A and B, show that GaN surface consists of uniform, oriented grains that coalesce well to each other. Cross-sectional bright-field TEM image, Fig. 5, demonstrates a highly ordered columnar structure of the film while selective area diffraction pattern, see inset, verifies that α-GaN is a dominant phase. (The TEM study is performed in a Joel 2000 microscope and the sample is prepared by mechanical polishing followed by ion milling.) These results suggest that nitridated GaAs serves as a nucleation layer for prismatic growth of c-oriented α-GaN. A weak diffraction from β-GaN can be attributed either to cubic grains at the GaN/GaAs interface, that can develop during the nitridation–annealing process, or to the small cubic inclusions randomly distributed throughout the film.

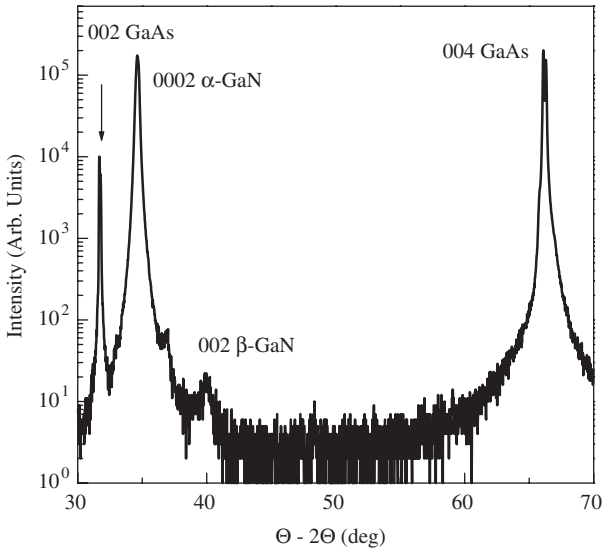

Fig. 3. XRD $\theta-2\theta$ scan of a ~2 μm thick GaN films grown on a GaAs substrate.

Fig. 6 shows low temperature (10 K) and room temperature (300 K) PL spectra. A 325-nm line of He–Cd laser is used for excitation. At room temperature one can see a relatively narrow, full-width at half-maximum ~76 meV, emission line at 3.2 eV and a broad band at ~2.3 eV. The 3.2 eV line can be assigned as a band-edge emission of β-GaN [12]. The low-energy band is often observed in GaN samples with a high dislocation density and is due to optical transitions involving defect levels in the forbidden energy band. The 10 K PL spectrum is dominated by emission lines at 3.26 and 3.16 eV. They are assigned as donor bound exciton and donor–acceptor pair (DAP) transitions of β-GaN [13,14]. A few LO–phonon replicas of DAP line are also evident. Thus, although film is

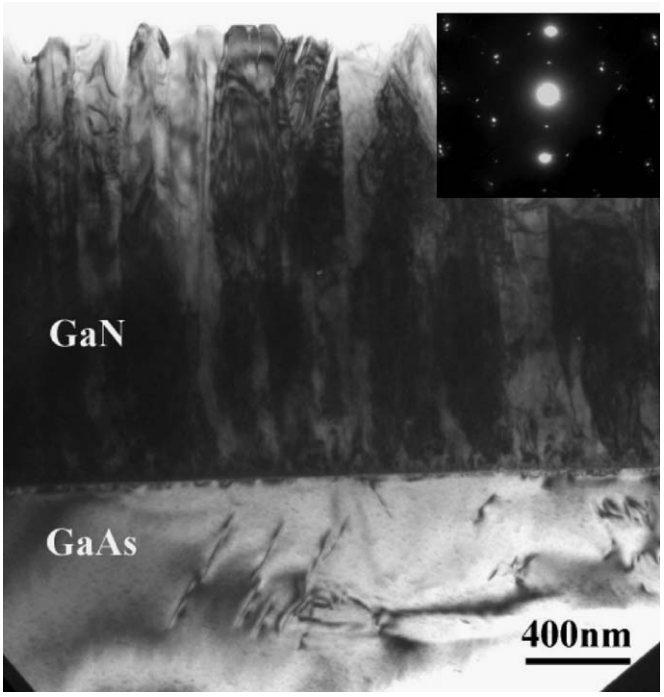

Fig. 5. Cross-sectional bright-field TEM image of a ~2 μm thick GaN film grown on a GaAs substrate. The inset is a selective area diffraction pattern.

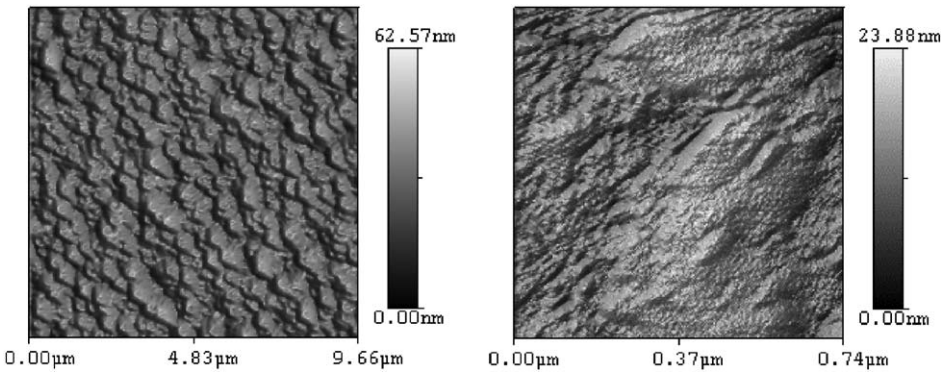

Fig. 4. AFM images of a ~2 μm thick GaN film grown on a GaAs substrate.

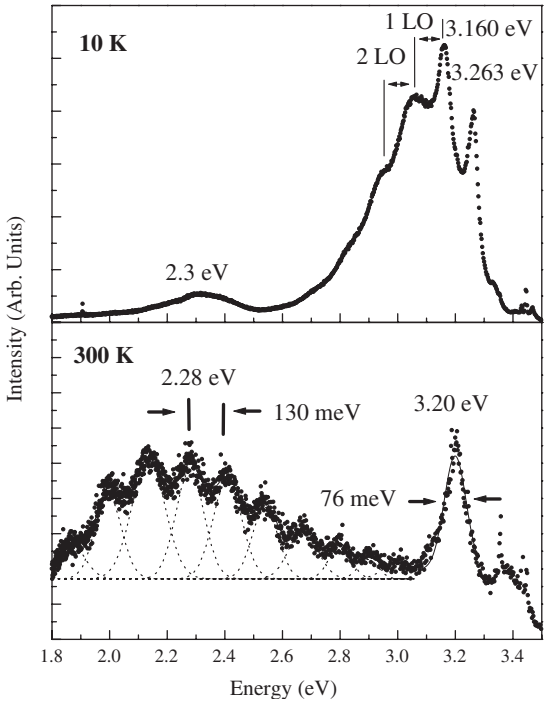

Fig. 6. Low (10 K) and room-temperature photoluminescence spectra of a ~2 μm thick GaN films grown on a GaAs substrate.

predominantly α-GaN, emission from cubic β-GaN inclusions dominates the spectrum.

The probing depth of PL is around 200 nm, while the GaN film is ~2 μm thick. Therefore, β-GaN inclusions, whose presence is demonstrated with XRD, are not localized at the substrate/epilayer interface but propagate throughout the film. It is suggested that since β-GaN has lower band gap than α-GaN (ΔE_g~0.2 eV) the inclusions can trap photogenerated carriers [15]. Then, they will serve as very efficient recombination sites in the expense of the dominant α-GaN.

In conclusion, GaN films are grown by MBE on [0 0 1] GaAs substrates. Their structural properties are studied with XRD and TEM; optical properties are evaluated by PL. Although the film grows as a c-oriented α-GaN, emission from cubic inclusion dominates the spectrum. We explain this fact by effective localization of photogenerated carriers at lower band gap β-GaN inclusions.

The work is supported by ONR (Dr. C.E.C. Wood).

References

[1] Mohammad SN, Salvador AA, Morkoc H. Proc IEEE 1995;83:1306.
[2] Fen R, Zolper JC. Wide Bandgap Electronic Devices. Singapore: World Scientific; 2003.
[3] Jiang HX, Lin JY. Opto-Electron Rev 2002;10:271.
[4] Brandt O, Muralihadharan R, Thamm A, Waltereit P, Ploog KH. Appl Surf Sci 2001;175:419.
[5] Brandt O, Yang H, Trampert A, Wassermeier M, Ploog KH. Appl Phys Lett 1997;71:473.
[6] Sung LW, Lin HH, Chia CT. J Cryst Growth 2002;241:320.
[7] Kimura R, Suzuki T, Ouchi M, Ishida K, Takahashi K. J Cryst Growth 2005;278:411.
[8] Okumura H, Hamaguci H, Feuillet G, Ishida Y, Yoshida S. Appl Phys Lett 1998;72:3056.
[9] Bell A, Ponce FA, Novikov SV, Foxon CT, Harrison I. Appl Phys Lett 2001;79:3239.
[10] Maksimov O, Fisher P, Du H, Skowronski M, Heydemann VD. In: North American MBE Conference, Santa Barbara, CA, 2005.
[11] Wasilewski ZR, Baribeau JM, Beaulieu M, Wu X, Sproule GI. J Vac Sci Technol B 2004;23:1534.
[12] Zinovev NN, Adrianov AV, Andrianov BY, Averbukh BY, Yarosetskii ID, Cheng TS, et al. Semicond Sci Technol 1995;10:1117.
[13] Georkilas A, Androulidaki M, Tsagaraki K, Amimer K, Constantidis C, Pelekanos NT, et al. Phys Stat Sol A 1999;176:525.
[14] Strauss U, Tews H, Riechert H, Averbeck R, Schienle M, Jobst B, et al. MRS Internet J Nitride Semicond Res 1996;1:44.
[15] Mah KW, Mosnier JP, MgGlynn E, Henty MO, O'Mahony D, Luney JG. Appl Phys Lett 2002;80:3301.